Heterodyne detection using spectral line pairing for spectral phase encoding optical code division multiple access and dynamic dispersion compensation

Yi Yang,* Mark Foster, Jacob B. Khurgin, and A. Brinton Cooper

[1]*Department of Electrical and Computer Engineering, The Johns Hopkins University 3400 N. Charles St, Barton 105, Baltimore, Maryland 21218, USA*

[*]*yyang30@jhu.edu*

Abstract: A novel coherent optical code-division multiple access (OCDMA) scheme is proposed that uses spectral line pairing to generate signals suitable for heterodyne decoding. Both signal and local reference are transmitted via a single optical fiber and a simple balanced receiver performs sourceless heterodyne detection, canceling speckle noise and multiple-access interference (MAI). To validate the idea, a 16 user fully loaded phase encoded system is simulated. Effects of fiber dispersion on system performance are studied as well. Both second and third order dispersion management is achieved by using a spectral phase encoder to adjust phase shifts of spectral components at the optical network unit (ONU).

OCIS codes: (060.0060) Fiber optics and optical communications; (060.5060) Phase modulation; (060.4230) Multiplexing; (320.5540) Pulse shaping; (060.1660) Coherent communications.

References and links

1. A. B. Cooper, J. B. Khurgin, S. M. Xu, and J. U. Kang, "Phase and polarization diversity for minimum MAI in OCDMA networks," IEEE J. Sel. Top. Quantum Electron. **13**(5), 1386–1395 (2007).
2. X. Wang and N. Wada, "Spectral phase encoding of ultra-short optical pulse in time domain for OCDMA application," Opt. Express **15**(12), 7319–7326 (2007).
3. X. Wang, Z. S. Gao, N. Kataoka, and N. Wada, "Time domain spectral phase encoding/DPSK data modulation using single phase modulator for OCDMA application," Opt. Express **18**(10), 9879–9890 (2010).
4. D. Zaccarin and M. Kavehrad, "An optical CDMA system based on spectral encoding of LED," IEEE Photon. Technol. Lett. **5**(4), 479–482 (1993).
5. M. Kavehrad and D. Zaccarin, "Optical code-division-multiplexed systems based on spectral encoding of noncoherent sources," J. Lightwave Technol. **13**(3), 534–545 (1995).
6. C. F. Lam, D. T. K. Tong, M. C. Wu, and E. Yablonovitvh, "Experimental demonstration of bipolar optical CDMA system using a balanced transmitter and complementary spectral encoding," IEEE Photon. Technol. Lett. **10**(10), 1504–1506 (1998).
7. P. C. Teh, P. Petropoulos, M. Ibsen, and D. J. Richardson, "A comparative study of the performance of seven and 63-chip optical code-division multiple-access encoders and decoders based on superstructured fiber Bragg gratings," J. Lightwave Technol. **19**(9), 1352–1365 (2001).
8. X. Wang, K. Matsushima, A. Nishiki, N. Wada, and K. Kitayama, "High reflectivity superstructured FBG for coherent optical code generation and recognition," Opt. Express **12**(22), 5457–5468 (2004).
9. C. C. Chang, H. P. Sardesai, and A. M. Weiner, "Code-division multiple-access encoding and decoding of femtosecond optical pulses over a 2.5-km fiber link," IEEE Photon. Technol. Lett. **10**(1), 171–173 (1998).
10. A. Agarwal, P. Toliver, R. Menendez, T. Banwell, J. Jackel, and S. Etemad, "Spectrally efficient six-user coherent OCDMA system using reconfigurable integrated ring resonator circuits," IEEE Photon. Technol. Lett. **18**(18), 1952–1954 (2006).
11. J. Cao, R. G. Broeke, N. K. Fontaine, C. Ji, Y. Du, N. Chubun, K. Aihara, A.-V. Pham, F. Olsson, S. Lourdudoss, and S. J. B. Yoo, "Demonstration of spectral phase O-CDMA encoding and decoding in monolithically integrated arrayed-waveguide-grating-based encoder," IEEE Photon. Technol. Lett. **18**(24), 2602–2604 (2006).

#169420 - $15.00 USD Received 29 May 2012; revised 9 Jul 2012; accepted 10 Jul 2012; published 18 Jul 2012

12. W. H. C. de Krom, "Impact of laser phase noise on the performance of a 3 × 3 phase and polarization diversity optical homodyne DPSK receiver," J. Lightwave Technol. **8**(11), 1709–1715 (1990).
13. Y. Yang, A. B. Cooper, J. B. Khurgin, and J. U. Kang, "Robustness of coherent SPE-OCDMA to combined dispersion impairments," Proc. CLEO, Baltimore, (2011).
14. T. Mizuno, T. Kitoh, T. Saida, Y. Inoue, M. Itoh, T. Shibata, Y. Hibino, and Y. Hida, "Low-loss 1.5%-Δ arrayed waveguide grating with narrow laterally tapered spotsize converter," Electron. Lett. **37**(24), 1452–1454 (2001).
15. Y. Yang, A. B. Cooper III, J. B. Khurgin, and J. Kang, "Sequences for impairment mitigation in coherent SPE-OCDMA," Proc. SPPCOM Topic Meeting Advanced Photonics Conference, Toronto, (2011).
16. A. Weiner, *Ultrafast Optics* (John Wiley & Sons, 2009).
17. C. C. Chang, H. P. Sardesai, and A. M. Weiner, "Dispersion-free fiber transmission for femtosecond pulses by use of a dispersion-compensating fiber and a programmable pulse shaper," Opt. Lett. **23**(4), 283–285 (1998).
18. S. Shen and A. M. Weiner, "Complete dispersion compensation for 400-fs pulse transmission over 10-km fiber link using dispersion compensating fiber and spectral phase equalizer," IEEE Photon. Technol. Lett. **11**(7), 827–829 (1999).
19. P. Toliver, A. Agarwal, R. Menendez, J. Jackel, and S. Etemad, "Optical code division multiplexing for confidentiality at the photonic layer in metro networks and beyond," Proc. SPIE **7235**, 723506, 723506-10 (2009).
20. J. Chen, Q. Zhang, C. Yu, X. Xin, Y. Shi, F. Deng, and C. Jin, "40Gbit/s PON over OCDMA uplink using DQPSK/OOK orthogonal re-modulation," Proc. SPIE **7848**, 784837, 784837-8 (2010).
21. Z. Gao, X. Wang, N. Kataoka, and N. Wada, "Demonstration of a two-user time domain spectral phase enoding OCDMA system with variable bandwidth spectrum shaper based decoder," Microw. Opt. Technol. Lett. **53**(8), 1879–1882 (2011).
22. S. J. Yoo, J. P. Heritage, V. J. Hernandez, R. P. Scott, W. Cong, N. K. Fontaine, R. G. Broeke, J. Cao, S.-W. Seo, J.-H. Baek, F. M. Soares, Y. Du, C. Yang, W. Jiang, K. Aihara, Z. Ding, B. H. Kolner, S. Anh-Vu Pham, S. Lin, F. Olsson, S. Lourdudoss, K. Y. Liou, S. N. Chu, R. A. Hamm, B. Patel, W. S. Hobson, J. R. Lothian, S. Vatanapradit, L. A. Gruezke, W. T. Tsang, M. Shearn, and A. Scherer, "Spectral phase encoded time spread optical code division multiple access technology for next generation communication networks [Invited]," J. Opt. Netw. **6**(10), 1210–1227 (2007).

1. Introduction

Code-division multiple access (CDMA) is widely used in wireless communications because of its spectral efficiency, system capacity, signal quality, security, and flexibility [1]. It is believed that optical CDMA (OCDMA) would bring CDMA benefits to fiber optic communications networks, in particular to local passive optical networks (PON's). In OCDM, users share a given transmission bandwidth, and uniquely encoded signals travel through the same transmission medium. The inherent attributes of OCDMA include asynchronous transmission, communications security, soft capacity on demand, protocol transparency, simplified network management, and flexibility [1,2]. A number of attempts at OCDMA have been made; however performance has been limited by speckle noise and multiple access interference (MAI) generated in receivers that are not fully coherent.

Existing and proposed OCDMA schemes are usually classified as either coherent or incoherent [3]. Coherent reception implies the ability to measure both amplitude and phase of the received optical signal. Since direct optical phase measurement is generally unfeasible, various interferometric techniques have been adopted in an attempt to gain the OCDMA advantage without fully coherent reception [1]. Incoherent OCDMA usually adopts spectral intensity encoding of an optical code (OC) onto the line spectrum of an incoherent source such as a light emitting diode [4], a superluminescent diode [5], or a multiwavelength laser array [6] source. While relatively simple to implement, incoherent OCDMA lacks an effective means to reject speckle and MAI compared to coherent OCDMA [1]. In what is commonly referred to as coherent OCDMA, the encoding is fully coherent, and waveforms can be generated by performing encoding in the time domain through a superstructured fiber Bragg grating (SSFBG) [7,8]; or by performing phase or amplitude encoding in the frequency domain [2], adopting either programmable liquid crystal modulators (LCM) [9], micro-ring resonators [10], or arrayed wave-guild gratings (AWG) [11]. A recent development in spectral phase encoding time spread OCDMA (SPECTS-OCDMA) uses two fibers with opposite dispersion values, first to stretch the short optical pulse in the time domain, then to spectrally phase encode, and finally to compress the pulse with the second fiber [2]. While

#169420 - $15.00 USD Received 29 May 2012; revised 9 Jul 2012; accepted 10 Jul 2012; published 18 Jul 2012

encoding for these systems is fully coherent, the detection schemes are not truly coherent in the sense that orthogonal codes do not produce zero energy at the detector, but only shift that energy in the time domain, causing speckle and MAI to limit system performance significantly. The high autocorrelation peak also requires a fast nonlinear threshold detector to capture the ultra-short optical pulse. Both time spread OCDMA (TS-OCDMA) and SPECTS-OCDMA require a fast phase or amplitude modulator [3], and the auto-correlation in TS-OCDMA produces not only a sharp peak, but also low level sidelobes [2].

Recently, we proposed a new coherent OCDMA combining spectral phase encoding (SPE) and phase and polarization diversity (PPD) [1] detection. This scheme inherits the attributes for SPE-OCDMA, while making obsolete the requirement for a phase-locked loop (PLL) and nonlinear threshold. It has been shown that the system is able to eliminate MAI and speckle noise and achieve high spectral efficiency [1]. Unfortunately, such a homodyne system requires has a complex receiver design and requires two fibers to convey the reference comb and signal comb separately [1,12,13].

This work proposes, and validates through simulation, a novel heterodyne scheme that pairs an encoded optical comb with an unencoded reference comb that is spectrally offset by the bit rate, resulting in single fiber transmission and a simple sourceless receiver with one fourth the number of detectors of a similar scheme [1]. True coherent processing and cancellation of speckle and MAI are realized while eliminating the need for a PLL and fast nonlinear threshold. Furthermore, this work proposes applying phase shifts computed with Fourier synthesis techniques as an effective technique to manage total dispersion in coherent OCDMA.

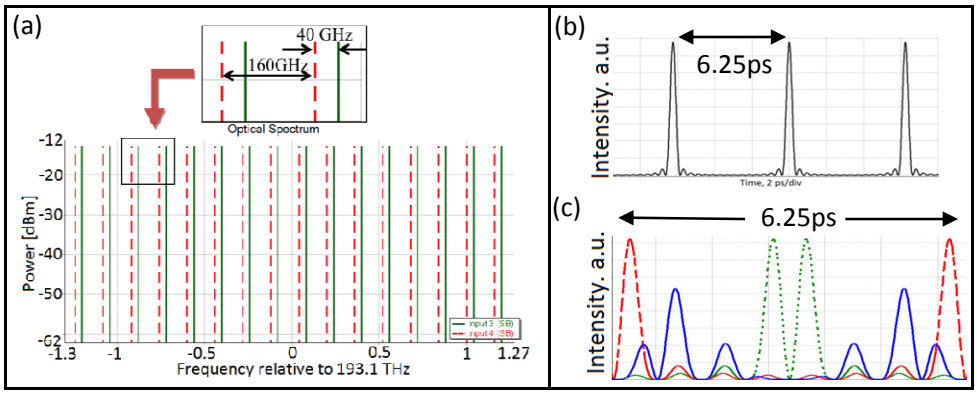

Fig. 1. (a). Frequency comb for reference and signal. (b) Unencoded signal or reference pulse at 160 GHz. (c) Encoded pulse shape for Hadamard sequence 9,10, and 15.

2. Proposed SPE scheme

As in [1], all optical signals are sourced from a single mode-locked laser (MLL) with a repetition rate $1/T$. Filtering with an arrayed waveguide grating (AWG) [14] produces two combs, each with a line spacing of $4\Delta f = 4/T$. The combs are offset from one another by Δf as in Fig. 1(a), depicting the signal comb as red dashed lines and the reference comb as green solid lines. Each user's signal comb is spectrally phase encoded (SPE) by a symbol from a distinct sequence of length N. In the receiver, heterodyne reception of signal and reference combs produces a data modulated stream at Δf. For $\Delta f = 40$ GHz, Fig. 1(b) shows that the period of the filtered comb signal is 6.25 ps (instead of 25 ps) due to the selected spectral line spacing. An example of an SPE waveform is shown in Fig. 1(c). Further, in our scheme, crosstalk from AWG channels cannot degrade performance because even the

#169420 - $15.00 USD Received 29 May 2012; revised 9 Jul 2012; accepted 10 Jul 2012; published 18 Jul 2012

strongest crosstalk component, generated from adjacent AWG channels, lies well outside the bandwidth of the filter at the balanced detector output.

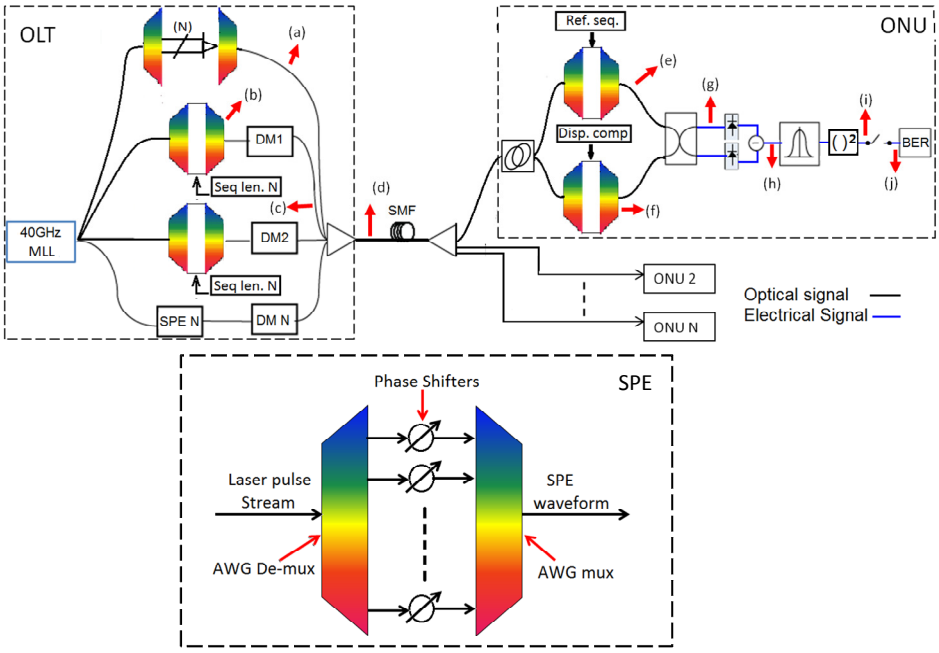

Fig. 2. Proposed system and spectral phase encoding (SPE) using AWGs and phase shifters.

Let the sequence of user m be $(C_m^{(1)}, C_m^{(2)}, ..., C_m^{(N)})$. The resulting phase encoded electrical fields of the composite signal and reference are given by Eqs. (1) and (2) respectively:

$$E_S(t) = \sqrt{P_S} \sum_{m=1}^{M} A_m e^{j\omega_o t} \sum_{i=-N/2}^{N/2-1} C_m^{(i)} e^{j4i\Delta\omega t} \tag{1}$$

$$E_l(t) = \sqrt{P_{LO}}\, e^{j\omega_o t} \sum_{i=-N/2}^{N/2-1} C_l^{(i)} e^{j(4i+1)\Delta\omega t}, \tag{2}$$

where M is the number of users; subscripts S and LO denote the user and reference signals; P and ω_0 are optical power and carrier angular frequency; A_m is the data bit (0 or 1) for the m^{th} user's signal; N is the length of the encoding sequence. $C_m^{(i)}$ and $C_l^{(i)}$ are respective values of the i^{th} chips of the signal and reference sequence; and the angular frequencies for the reference and information-bearing signals are $\omega_o + (4i+1)\Delta\omega$ and $\omega_0 + 4i\Delta\omega$, respectively (points (a) and (b) in Fig. 2). The pulse shapes of three of sixteen Hadamard sequence-encoded pulses are shown at (c) of Fig. 1. The dashed, dotted, and solid lines are pulse shapes encoded with the 9th, 10th, and 15th sequences respectively, and they exhibit distinct energy distributions across the bit interval. Table 1 shows the encoding sequences in terms of phase shifts at the AWG. The signals and reference light are multiplexed by a star coupler, and sent to up to $M = 16$ ONUs via a single fiber as at (d), Fig. 2.

Table 1. Encoder phase shifts corresponding to Hadamard sequences 9, 10, and 15.

Seq.																
9	0	0	0	0	0	0	0	0	π	π	π	π	π	π	π	π
10	0	π	0	π	0	π	0	π	π	0	π	0	π	0	π	0
15	0	0	π	π	π	π	0	0	π	π	0	0	0	0	π	π

#169420 - $15.00 USD Received 29 May 2012; revised 9 Jul 2012; accepted 10 Jul 2012; published 18 Jul 2012

At the ONU, the signal and reference comb are separated by an interleaver. The reference is encoded in an SPE (at (e), Fig. 2) by the sequence of the signal to be extracted from the received ensemble. A second SPE (at (f), Fig. 2) is used for dispersion compensation (see Section 4). Otherwise, the entire received ensemble is at (f). Both paths are joined at the hybrid coupler and subsequently to the balanced detector. The electrical fields entering the top ((g) of Fig. 2) and bottom of the detector are E_1 and E_2, respectively.

$$E_1 = \frac{E_l}{2} + j\frac{E_S}{2} \tag{3}$$

$$E_2 = j\frac{E_l}{2} + \frac{E_S}{2} \tag{4}$$

Each of the balanced detectors effectively multiplies the two signals and outputs P_1 and P_2 :

$$P_1 = \mid E_1 \mid^2 = \left| \frac{E_l}{2} + j\frac{E_S}{2} \right|^2 = \frac{1}{4}(\left|E_l\right|^2 + \left|E_S\right|^2 + jE_S E_l^* - jE_l E_S^*) \tag{5}$$

$$P_2 = \mid E_2 \mid^2 = \left| j\frac{E_l}{2} + \frac{E_S}{2} \right|^2 = \frac{1}{4}(\left|E_l\right|^2 + \left|E_S\right|^2 + jE_l E_S^* - jE_S E_l^*). \tag{6}$$

The power of the LO oscillator is

$$\mid E_l \mid^2 = \frac{P_{LO}}{4} \sum_{i=-N/2}^{N/2-1} \sum_{k=-N/2}^{N/2-1} F(4k\Delta\omega) C_l^{(i)} C_l^{(i+k)} e^{jk4\Delta\omega t}, \tag{7}$$

where $4\Delta\omega$ is a multiple of the beat frequency of the LO combs and $F(4k\Delta\omega)$ represents the frequency response of the detector. In the balanced detector, this term is canceled. The power of the signal, also containing the same beat frequencies $4\Delta\omega$, is:

$$\mid E_S \mid^2 = \frac{P_S}{4} \sum_{i=-N/2}^{N/2-1} \sum_{k=-N/2}^{N/2-1} \left[F(4k\Delta\omega) \sum_{m=1}^{M} \sum_{n=1}^{M} A_m A_n^* C_m^{(i)} C_n^{(i+k)} e^{jk4\Delta\omega t} \right]. \tag{8}$$

$\mid E_s \mid^2$ thus represents the speckle noise. In the proposed scheme, this term is completely cancelled out at the balanced detector, and the only remaining terms are the interference terms. The output (Fig. 2(h)) from the balanced detector is:

$$P = P_1 - P_2 = \frac{1}{2}\left(jE_S E_l^* + c.c. \right) \tag{9}$$

Substituting Eq. (1) and (2) into Eq. (9),

$$I(t) = \eta \frac{j}{2} \sqrt{P_{LO} P_S} \left[\sum_{m=1}^{M} A_m \sum_{i=-N/2}^{N/2-1} \sum_{k=-N/2}^{N/2-1} F[\left(4k \pm 1\right)\Delta\omega] C_m^{(i)} C_l^{(i+k)} e^{j(4k\pm1)\Delta\omega t} \right] + cc \tag{10}$$

where η is the detector responsively, and we have dropped the irrelevant $\pi/2$ phase shift. Complete cancellation of the speckle noise is the first salient feature of our scheme, differentiating it from all previous schemes. As one can see, the current spectrum contains frequency components centered around frequencies of all odd multiples of the repetition rate $(2n-1)\Delta\omega$. Higher frequencies are significantly suppressed by the detector response F and can be further eliminated by the low pass cut-off filter to leave only the lowest frequency term

#169420 - $15.00 USD Received 29 May 2012; revised 9 Jul 2012; accepted 10 Jul 2012; published 18 Jul 2012

$$I(t) \sim \eta\sqrt{P_{LO}P_S}\sum_{m=1}^{M} A_m \sum_{i=-N/2}^{N/2-1} C_m^{(i)} C_l^{(i)} e^{j\Delta\omega t} + cc \tag{11}$$

Having eliminated speckle noise, we eliminate MAI by taking full advantage of the sequence orthogonality that enables the decoder to produce a true autocorrelation (with both positive and negative terms) and achieve near-zero pairwise crosscorrelation between signals encoded with distinct sequences. The crosscorrelation is given by,

$$\sum_{i=-N/2}^{N/2-1} C_m^i C_\ell^i e^{j(\Delta\omega)t} = e^{j(\Delta\omega)t} \sum_{i=-N/2}^{N/2-1} C_m^i C_l^i = \begin{cases} Ne^{j(\Delta\omega)t}, & (m=l) \\ 0, & (m\neq l) \end{cases} \tag{12}$$

To the best of our knowledge, this perfect cancellation of MAI is a unique feature of this scheme and is a direct consequence of the heterodyne detection in which we correlate fields rather than intensities. Yet, note that this cancellation is achieved without phase or frequency locked loops and without using any ultrafast or nonlinear components. The detector should be able to handle the frequencies of about $1.5\Delta f$ (60 GHz in this example, or less in lower data rate schemes), while the system capacity is 16 × 40 = 640 Gbps and the total bandwidth is about 2500 GHz, much wider than the detector bandwidth.

All that remains is to move the signal [Eq. (11)] into the baseband, which can be accomplished by beating it with a 40 GHz signal from the recovered clock or simply by squaring it.

$$\left|I(t)\right|^2 \sim \eta^2 P_{LO} P_S A_m^2 N^2 \tag{13}$$

This resulting signal is sent to a 40 GHz integrate and dump receiver ((j) of Fig. 2) before entering the BER calculator. Note that, in the numerical examples, we are integrating over one period T, *i.e.,* four full periods of the phase encoded signal.

3. Back-to-back simulation and results

We simulate a stream of Gaussian-like optical pulses from a 1550 nm mode-locked laser (MLL) with a period of 25 ps and a pulse duration of 500 fs. The main lobe of the optical comb is spectrally flattened [1] to ensure full signal orthogonality. Figure 3(a) shows the reference comb and pulse train without phase encoding. In the optical line terminal (OLT), a SPE encodes each user's signal with a distinct length 16 Hadamard code (Fig. 2), producing the representation of Fig. 3(b). Following on-off keying (OOK) data modulation at 40 Gbps, each bit covers four SPE optical pulses, as shown in Fig. 3(c), which also shows the resulting spectral line broadening caused by the OOK.

In the fully loaded configuration of Fig. 3(d), sixteen users plus the unencoded reference are coupled into a single mode fiber (SMF) and sent across the network. In the ONU, an optical interleaver separates the reference comb and encodes it with the 10th user's sequence (Fig. 3(e)). The signal ensemble (Fig. 3(f)) passes through a 32 channel AWG that is used for dispersion compensation as discussed in Section 4, and signal processing proceeds as explained in Section 2. Typical output from one branch of the hybrid is at Fig. 3(g) where speckle noise is clearly visible. Both speckle and MAI are gone, however, when the two signals are subtracted (Fig. 3(h)). In fact, one can already discern the OOK data multiplied by the 40 GHz beat carrier. Following detection, squaring, and integrating to 40 GHz (Fig. 3(h) and 3(i)), the integrated sample (Fig. 3(j)) is sent to the BER calculator prior to dumping.

#169420 - $15.00 USD Received 29 May 2012; revised 9 Jul 2012; accepted 10 Jul 2012; published 18 Jul 2012

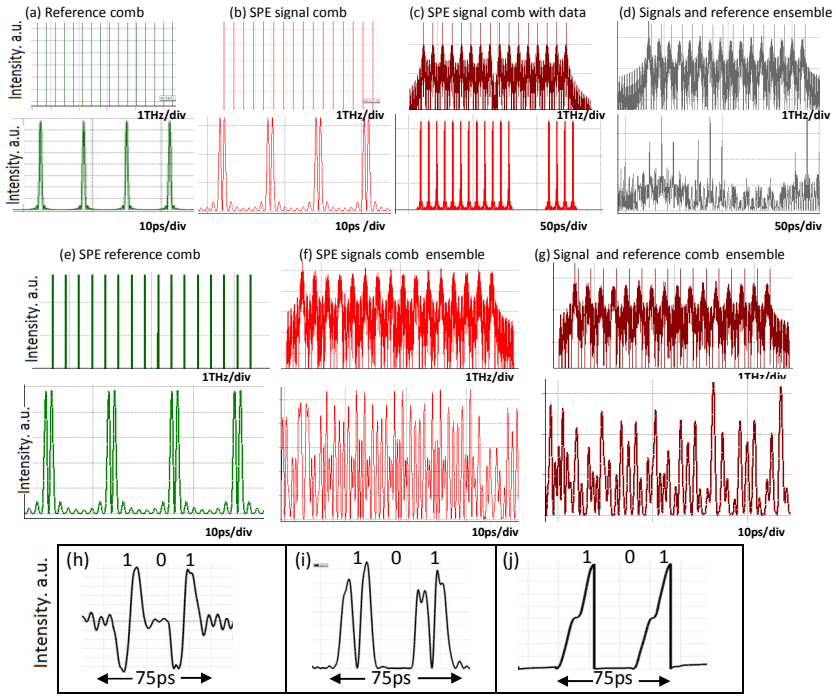

Fig. 3. Simulated signals for the proposed OCDMA system. The OLT is represented in (a) through (d); (e) to (j) are the simulated signals in the ONU. Index letters correspond to points in the diagram of Fig. 2. Note that, following the subtraction at (h), the speckle is gone.

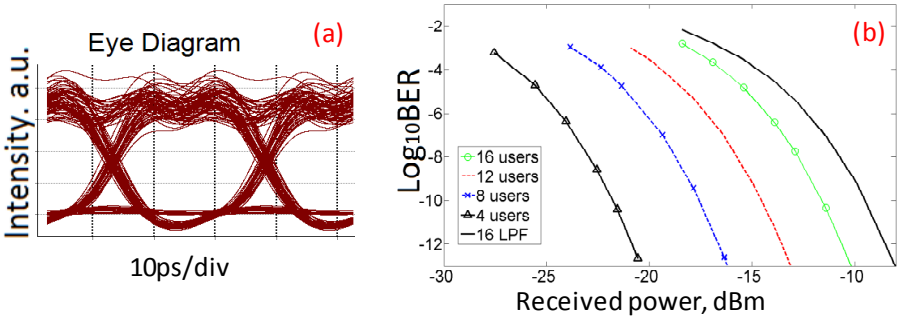

Fig. 4. Transmitting experiment. (a) Eye diagram for BER = 10^{-9}; (b) BER for four system load levels with integrate and dump and full loading with LPF. Received power is that which enters the ONU.

Table 2 shows that the required optical power to achieve a BER of 10^{-9} (Fig. 4(b)) compares favorably with previously proposed OCDMA systems and, in most cases, our proposed system uses spectrum more efficiently.

Table 2. Received optical power of proposed OCDMA schemes for 10^{-9} BER

# of Users	Individual user data rate	Received optical power for 10^{-9} BER	Ref.
5	40.0 Gb/s	–19.5 dBm	[20]
4	2.5 Gb/s	–27.5 dBm	[21]
4	10.0 Gb/s	–24.0 dBm	[22]
4	40.0 Gb/s	–23.0 dBm	Figure 4(b)

#169420 - $15.00 USD Received 29 May 2012; revised 9 Jul 2012; accepted 10 Jul 2012; published 18 Jul 2012

Replacing integrate and dump with a simple 40 GHz low pass filter (LPF) produces the eye diagram in Fig. 4(a). However, the tradeoff for simplicity is system performance. A fully loaded 16-user system with a LPF achieves a higher BER (black curve, Fig. 4(b)) compared to the integrator (green line with circles) at the same receiving power level. Performance vs system loading is shown as well.

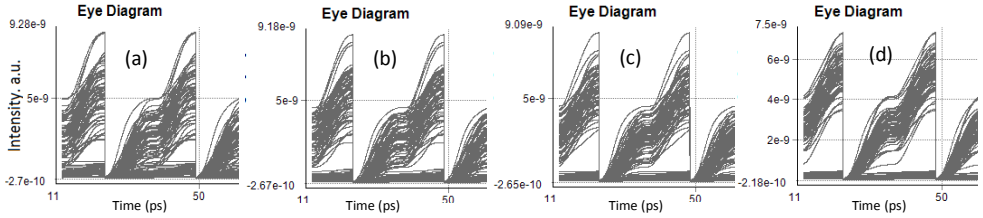

Fig. 5. Eye diagrams at the receiver for different system loads irrespective of whether the intended user is transmitting.

To display the full effect of data transmitted by all users, Fig. 5 shows the broadening of the eye for the 10^{th} user as system load is decreased from 16 to 4 users in increments of 4 ((a) through (d)) with an integrate and dump receiver, a received power of -18.4 dBm, and the transmission of distinct pseudorandom data by every user. By comparison, Fig. 6 shows eye diagrams for fully loaded systems for the 9^{th} and 15^{th} users respectively. In order to magnify the display, the ONU receiving power is set to –10 dBm.

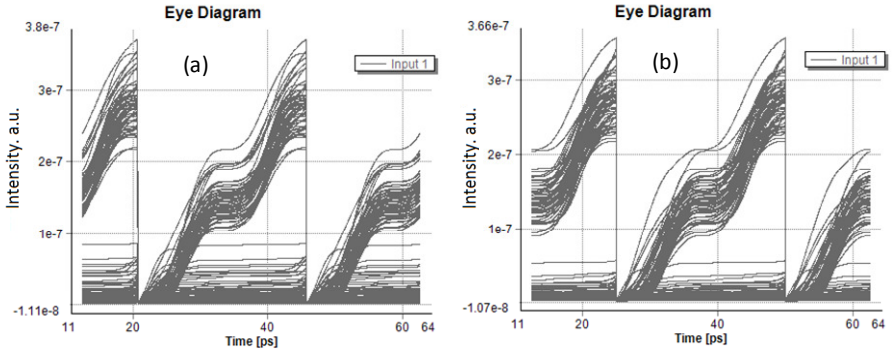

Fig. 6. Receiver eye diagram for the 9th and 15th encoding sequence.

4. Impact of the group velocity dispersion (GVD)

Fiber dispersion broadens the pulse in the temporal domain, leading to intersymbol interference (ISI) [1,15]. In addition, as the signal and reference combs travel through the fiber, dispersion adds extra phase to each spectral line, resulting in dispersion-induced MAI at the receiver. The BER vs. length of SMF of the uncompensated system at various loadings is shown in Fig. 7(a) for a received power of –10 dBm. The fiber dispersion is 17 ps/km/nm and the dispersion slope is 0.08 ps/km/nm^2. It has been demonstrated [16] that pulse shaping based on the Fourier synthesis method can be applied to dispersion compensation, but, to our knowledge, this method of compensation of a SPE/OCDMA waveform has not been demonstrated, and the obvious scheme of compensating the original 16 lines, is not helpful, as shown below, because the data modulation introduces additional spectral components and the frequency combs are no longer equally spaced lines of constant amplitude. Fourier synthesis can compensate both second and third order dispersion caused by SMF and dispersion mismatch, resulting in pulse compression and the elimination of (ISI) [17,18]. We propose implementing the Fourier synthesis pulse shaping method [16] by utilizing the ONU's phase

#169420 - $15.00 USD Received 29 May 2012; revised 9 Jul 2012; accepted 10 Jul 2012; published 18 Jul 2012

encoders for the application of corrective phase shifts, as computed below, to achieve dispersion compensation and mitigate MAI. The phase shift to be added to compensate for dispersion [18] is given by Eq. (14).

$$\phi(\Delta\omega) = -\frac{DL\lambda^2}{4\pi c}(\Delta\omega)^2 + \frac{LS\lambda^4}{24\pi^2 c^2}(\Delta\omega)^3 + \frac{DL\lambda^3}{12\pi^2 c^2}(\Delta\omega)^3 \qquad (14)$$

where D is the SMF dispersion coefficient, S is the dispersion slope, L is the optical fiber length, and $\lambda = c / f_0$ is the center wavelength of the optical pulse. Simulation results for a fully loaded system (16 users) show that applying phase corrections only to the original 16 spectral lines at a channel spacing of 160 GHz has no compensating effect. In fact, the 16 channel compensation curve of Fig. 7(a) is nearly congruent with the 16 user uncompensated curve. However, when 32 channels are compensated (by reducing the AWG channel spacing to 80 GHz at (f) of Fig. 2, thereby doubling the resolution) there is significant improvement, shifting the curve significantly toward the right in Fig. 7(a). To show exactly what phase shifts are added to the two AWGs, Fig. 7(b) gives the added phase for uncompensated residual dispersion provided by a 30 m length of SMF. Figure 7(c) shows the uncompensated phase encoded pulse; the compensated pulse shape is quite similar to the original shape in Fig. 7(d). In the above simulation, no dispersion compensated fiber (DCF) was assumed. It has been previously demonstrated [19] that an OCDMA system, combined with dispersion compensated SMF fiber is capable of transmitting signals for a total distance of 400 km. However, the combination of long distance SMF and DCF can introduce a small mismatch between second and third order dispersions. The proposed technique can be implemented to compensate this residual dispersion [17,18] for long haul SPE-OCDMA communication.

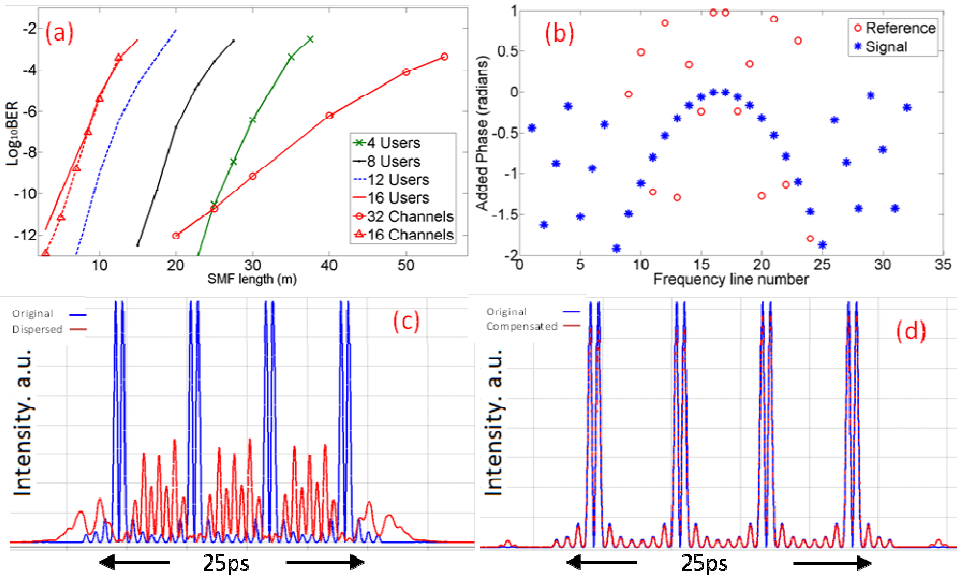

Fig. 7. (a) BER vs. Total Dispersion. (b) Added phase to spectral components. For the reference comb, the 10th Hadamard encoding sequence and dispersion compensation are both added, whereas only dispersion compensation phase is added for the signal comb. (c) Pulse shape without compensation and (d) with compensation.

5. Conclusion

We have proposed and analyzed a novel configuration for a coherent, spectrally phase encoded OCDMA system that, for the first time, completely cancels speckle noise and

#169420 - $15.00 USD Received 29 May 2012; revised 9 Jul 2012; accepted 10 Jul 2012; published 18 Jul 2012

multiple access interference. A simple balanced detector beats a locally encoded reference comb with the ensemble of data modulated OCDMA signals, cancelling speckle (beat) noise and MAI coherently, without the need for phase locked loops or fast, nonlinear detectors. Simulations have shown that error-free operation can be achieved with a fully loaded (16 users at 40 Gb/s each) with a spectral efficiency of ¼ bit/sec/Hz, which is very high for OCDMA. Because the receiver configuration is colorless and sourceless, our scheme is an excellent candidate for PONs and other applications involving large numbers of efficient, identical, low power units. In addition, we have implemented a non-obvious way to apply Fourier synthesis techniques to the compensation of residual dispersion, thus easing certain implementation challenges.

Acknowledgments

This work was supported by the US National Science Foundation under Grant ECCS-0925470 and funded under the American Recovery and Reinvestment Act of 2009 (ARRA). The simulation platform is VPItransmissionMaker Optical Systems (www.vpiphotonics.com).

#169420 - $15.00 USD Received 29 May 2012; revised 9 Jul 2012; accepted 10 Jul 2012; published 18 Jul 2012